AD-B191 758 OPTIMIZATION OF AIRFOILS FOR HYPERSONIC FLIGHT(U) 1/1
AERONAUTICAL RESEARCH ASSOCIATES OF PRINCETON INC NJ
C DONALDSON ET AL. 1 JUL 60 XD-XD

UNCLASSIFIED DTIC

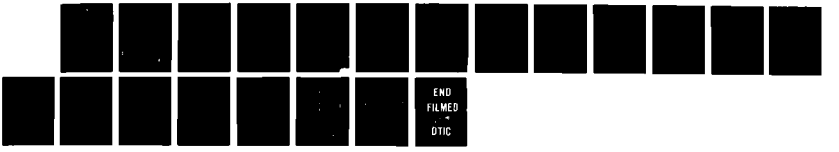

AIIM

Association for Information and Image Management

1100 Wayne Avenue, Suite 1100
Silver Spring, Maryland 20910

301/587-8202

Centimeter

1 2 3 4 5 6 7 8 9 10 11 12 13 14 15 mm

1 2 3 4 5

Inches

1.0 1.1 1.25 1.4 1.6 1.8 2.0 2.2 2.5 2.8 3.2 3.6 4.0 4.5 5.0 5.6

MANUFACTURED TO AIIM STANDARDS

BY APPLIED IMAGE, INC.

OPTIMIZATION OF AIRFOILS FOR HYPERSONIC FLIGHT

by

Coleman duP. Donaldson and K. Evan Gray
Aeronautical Research Associates of Princeton, Inc.

Presented at the
IAS National Summer Meeting
Los Angeles, California
June 28 - July 1, 1960

IAS Paper No. 60-65

Member Price - - - - $0.50
Nonmember Price - $1.00

OPTIMIZATION OF AIRFOILS FOR HYPERSONIC FLIGHT

by

Coleman duP. Donaldson

and

K. Evan Gray

Aeronautical Research Associates of Princeton, Inc.

ABSTRACT

Because of the extreme aerodynamic heating rates that exist for hypersonic flight at low altitudes, steady hypersonic flight is only possible at very high altitudes. In general, the greater the Mach number the greater the altitude required. Thus, the greater the hypersonic Mach number the lower the flight Reynolds number. For high L/D vehicles, this requirement of low flight Reynolds number means that the viscous drag may become an important fraction of the total drag of the vehicle. In the past, theoretical approaches to the design high L/D supersonic vehicles have needed to consider only the pressure drag in finding the shape of a body having a minimum drag for a given lift. In view of the possibility of the viscous drag becoming a more important fraction of the total drag for some hypersonic configurations, the present paper attacks the problem of the body shape required for minimum drag when both viscous and pressure drag are considered. In the present paper only the two-dimensional problem is considered.

In the first portion of the paper, the Karman momentum integral for boundary layer growth is cast into a form which permits an expression for the local skin friction at a particular point on a body to be derived in terms of an integral which depends on the distribution of body shape up to that point. This expression for the local viscous drag is then combined with the usual expression for the local pressure drag so that in the case of two-dimensional flow, by a suitable transformation of variables, the expression for the total drag of the body can be put into an integral form which may be treated by classical methods of the calculus of variations.

The second portion of the paper deals with a discussion of solutions to the minimization problem posed above subject to the constraint of fixed lift. Several interesting general conculsions may be drawn concerning the way in which lift must be distributed on a body for optimum drag when the Reynolds number is such that viscous drag is an appreciable fraction of the total drag.

INTRODUCTION

In the past, aeronautical engineers have in general been concerned with the aerodynamic characteristics of wings and bodies for which the Reynolds numbers to be encountered in flight were of the order of millions or tens of millions. Thus, in the classical aerodynamic problems of finding optimum airfoil and body shapes, it has been customary to neglect the local distribution of viscous forces and seek those shapes which yield the optimum distribution of pressure forces (see for example Refs. 1, 2, and 3). The very high aerodynamic heating rates which are encountered upon hypersonic vehicles at low altitudes have forced the designer of such vehicles to consider flight at very great altitudes. In view of the fact that at very great altitudes the Reynolds number may no longer be of the order of millions, the viscous drag of hypersonic vehicles flying at large altitudes may be an appreciable percentage of their total drag. It would therefore seem desirable to examine in some detail the classical problems of aerodynamic shape optimization where consideration is given to both viscous and pressure forces. In what follows, a portion of the results of such a study carried out for the Grumman Aircraft Engineering Corporation

is presented. The problem treated is that of the shape of a two-dimensional, sharp, hypersonic airfoil having minimum drag for a specified lift when both pressure and viscous forces are considered.

The paper is divided into essentially two parts. In the first part, an expression for the local skin friction is derived which, when added to the usual expression for the local pressure drag, allows the expression for the total drag to be cast into a form suitable for treatment by standard methods of the calculus of variations. The second portion of the paper discusses the solution of the drag minimization problem formulated in the first section.

1. *EXPRESSION FOR TOTAL DRAG*

BOUNDARY LAYER MOMENTUM EQUATION

In order to obtain an expression for the local viscous contribution to the total drag of an airfoil, it is necessary to compute the growth of the boundary layer as it passes over the surface of the airfoil. This growth may in general be found by integrating the Karman Momentum equation. For our purpose, that is for the growth of the boundary layer on a two-dimensional airfoil, the

Karman Momentum equation may be written

$$(1) \qquad \frac{d\delta_{**}}{ds} + \frac{\delta_{**}}{u_e}\left(2 + \frac{\delta_*}{\delta_{**}}\right)\frac{du_e}{ds} + \frac{\delta_{**}}{\rho_e}\frac{d\rho_e}{ds} = \frac{\tau_w}{\rho_e u_e^2}$$

where the variable s is measured along the surface of the airfoil in the flow direction, ρ and u are the fluid density and velocity, τ_w is the local wall shear, and the subscript e denotes conditions at the edge of the boundary layer. The quantities δ_* and δ_{**} are the boundary layer desplacement and momentum thicknesses respectively, namely

$$(2) \qquad \delta_* = \delta \int_0^1 \left(1 - \frac{\rho u}{\rho_e u_e}\right) d\left(\frac{n}{\delta}\right)$$

and

$$(3) \qquad \delta_{**} = \delta \int_0^1 \frac{\rho u}{\rho_e u_e}\left(1 - \frac{u}{u_e}\right) d\left(\frac{n}{\delta}\right)$$

Here n is measured normal to the airfoil surface and δ is the total boundary layer thickness.

In order to integrate Equation (1) it is necessary to evaluate the integrals given in Equations (2) and (3). This in turn requires a knowledge of the boundary layer velocity and density profiles. In regard to the density

profiles, it will be assumed that (a) the pressure gradient in the flow direction $\partial p/\partial s$ is small, (b) the Prandtl number is unity, (c) the medium is an ideal gas obeying the perfect gas law, and (d) that the usual boundary layer assumption of constancy of pressure through the boundary layer holds. These assumptions permit us to write

$$(4) \qquad \rho RT = p = p_e = \rho_e RT_e$$

and

$$(5) \qquad T = T_w + (T_e^0 - T_w)(u/u_e) - (T_e^0 - T_e)(u/u_e)^2$$

Here p and T are, as usual, pressure and temperature and the subscript w refers to stagnation conditions. In regard to the velocity distribution in the boundary layer which must be used in Equations (2) and (3), we are actually permitted a fair degree of latitude. In view of the assumption that the pressure gradient in the stream direction is small we may reasonably assume that the boundary layer profile $u/u_e = f(n/\delta)$ is fixed. The choice of this function is in our case somewhat arbitrary, for it has been found in the past that insofar as evaluating the local skin friction at a point is concerned,

rather unimportant variations are found by changing the function $f(n/\delta)$. Thus for simplicity in what follows we choose a straight line profile, namely

$$u/u_e = n/\delta \tag{6}$$

Use of Equations (4), (5), and (6) permit us to write the density distribution in the boundary layer as

$$\frac{\rho}{\rho_e} = \left[\frac{T_w}{T_e} + \left(\frac{T_e^0}{T_e} - \frac{T_w}{T_e}\right)\frac{n}{\delta} - \left(\frac{T_e^0}{T_e} - 1\right)\left(\frac{n}{\delta}\right)^2\right]^{-1} \tag{7a}$$

or in terms of the local Mach number M_e

$$\frac{\rho}{\rho_e} = \left[\frac{T_w}{T_e} + \left(1 + \frac{\gamma - 1}{2} M_e^2 - \frac{T_w}{T_e}\right)\frac{n}{\delta} - \frac{\gamma - 1}{2} M_e^2 \left(\frac{n}{\delta}\right)^2\right]^{-1} \tag{7b}$$

If Equations (6) and (7b) are substituted into Equations (2) and (3), it can be seen that δ_*/δ and δ_{**}/δ are functions of T_w/T_e, M_e, and γ which in turn are known functions of s depending on the body shape.

We may also use Equation (6) to write the right hand side of Equation (1) as

$$\frac{\tau_w}{\rho_e u_e^2} = \frac{\mu_w}{\rho_e u_e}\left(\frac{\delta_{**}}{\delta}\right)\left(\frac{1}{\delta_{**}}\right) \tag{8}$$

In view of Equation (8), Equation (1) may be rewritten as

$$\frac{d\delta_{**}^2}{ds} + \delta_{**}^2\left[\left(2 + \frac{\delta_*}{\delta_{**}}\right)\frac{2}{u_e}\frac{du_e}{ds} + \frac{2}{\rho_e}\frac{d\rho_e}{ds}\right] = \frac{2\mu_w}{\rho_e u_e}\left(\frac{\delta_{**}}{\delta}\right) \tag{9}$$

Equation (9) may be integrated explicitly to find the momentum thickness on a given body shape. However, the resulting expression is rather complicated due to the dependence of the terms δ_*/δ_{**} and δ_*/δ on s. Fortunately, for hypersonic flows Equation (9) may be put into a particularly simple form.

HYPERSONIC MOMENTUM EQUATION

If for the case of hypersonic flow, we assume that $T_e/T_e^0 \ll 1$ and that the surface of the wing is sufficiently cooled so that we may neglect T_w/T_e^0 in comparison with unity, then we may write

$$\frac{\rho}{\rho_e} = \frac{T_e}{T_e^0}\left[\frac{T_w}{T_e^0} + \frac{n}{\delta} - \left(\frac{n}{\delta}\right)^2\right]^{-1} \tag{10}$$

Inserting this result into Equations (2) and (3) and using Equation (6) one obtains

$$\frac{\delta_*}{\delta} \simeq 1 \tag{11}$$

and

$$(12) \qquad \frac{\delta_{**}}{\delta} \simeq \frac{T_e}{T_e^0}\left[1 - \frac{T_w}{T_e^0} \ln \frac{T_e^0}{T_w}\right] = \frac{T_e}{T_e^0}(1 - \alpha)$$

The quantity $\alpha = (T_w/T_e^0)\ln(T_e^0/T_w)$ will for our purposes be, in general, a small quantity. The behavior of α as a function of T_w/T_e^0 is plotted in Figure 1.

Using the above results, the factor $(2 + \delta_*/\delta_{**})$ in Equation (9) can be written

$$(13) \qquad 2 + \frac{\delta_*}{\delta_{**}} = 2 + \frac{T_e^0}{T_e}\frac{1}{(1 - \alpha)} \simeq \frac{T_e^0}{T_e}\frac{1}{(1 - \alpha)}$$

The remaining part of this term from Equation (9) is $(2/u_e)(du_e/ds)$, which may be transformed in the following manner. Since

$$(14) \qquad c_p T_e^0 = c_p T_e + \frac{1}{2} u_e^2 \simeq \frac{1}{2} u_e^2$$

and

$$(15) \qquad c_p dT_e = - u_e du_e$$

we have

$$(16) \qquad \frac{2}{u_e}\frac{du_e}{ds} \simeq - \frac{1}{T_e^0}\frac{dT_e}{ds}$$

Using Equations (13) and (16) we have

$$(17) \qquad \left(2 + \frac{\delta_*}{\delta_{**}}\right)\frac{2}{u_e}\frac{du_e}{ds} = - \frac{1}{(1 - \alpha)}\frac{1}{T_e}\frac{dT_e}{ds}$$

With this result the Karman Momentum equation (Equation (9)) becomes for hypersonic flow

$$(18) \qquad \frac{d\delta_{**}^2}{ds} + \delta_{**}^2\left[\frac{2}{\rho_e}\frac{d\rho_e}{ds} - \frac{1}{(1 - \alpha)}\frac{1}{T_e}\frac{dT_e}{ds}\right] = \frac{2\mu_w}{\rho_e u_e}\frac{T_e}{T_e^0}(1 - \alpha)$$

If the wall temperature is assumed constant so that α and thus also μ_w are independent of s then Equation (18) may be integrated explicitly to obtain

$$(19) \qquad \delta_{**}^2 = \frac{2(1 - \alpha)\mu_w T_e^{1/1-\alpha}}{\rho_e^2 T_e^0}\int_0^s \frac{\rho_e ds}{u_e T_e^{\alpha/1-\alpha}}$$

Here we have assumed a sharp body so that the initial boundary layer thickness is zero. The local wall shear τ_w may now be found using Equations (8), (12) and (19),

one obtains

$$(20) \qquad \tau_w = \left[\frac{\gamma(1-\alpha)}{(\gamma-1)} \frac{\mu_w p_e^2}{T_e^{1/1-\alpha}}\right]^{\frac{1}{2}} \left[\int_0^s \frac{p_e ds}{u_e T_e^{1/1-\alpha}}\right]^{-\frac{1}{2}}$$

If we make Equation (20) non-dimensional by dividing τ_w by $\rho_\infty V_\infty^2$ (where the subscript ∞ refers to undisturbed free stream conditions) and if we note that for sharp bodies at hypersonic speeds $u_e \simeq V_\infty$ we obtain

$$(21) \quad \frac{\tau_w}{\rho_\infty V_\infty^2} = \left[\frac{\gamma(1-\alpha)}{(\gamma-1)}\left(\frac{\mu_w}{\rho_\infty V_\infty c}\right)\left(\frac{p_\infty}{\rho_\infty V_\infty^2}\right)\left(\frac{p_e}{p_\infty}\right)^2\left(\frac{T_e}{T_\infty}\right)^{\frac{-1}{1-\alpha}}\right]^{\frac{1}{2}} \left[\int_0^{\frac{s}{c}} \frac{p_e}{p_\infty}\left(\frac{T_e}{T_\infty}\right)^{\frac{-1}{1-\alpha}} d\left(\frac{s}{c}\right)\right]^{-\frac{1}{2}}$$

when the variable s has been made non-dimensional by means of the chord length c.

Up to this point our analysis has been quite general. In order now to demonstrate how Equation (21) may be used in a variational analysis for the shape giving minimum drag for a given lift, it is necessary to relate the

terms p_e/p_∞ and T_e/T_∞ in Equation (21) to the local surface slope of the body under consideration. A number of assumptions have been made relating the local pressures and temperatures to the local body slope and the resulting optimum airfoils derived. For the purposes of this paper, the assumptions we shall use to demonstrate the method are as follows: (a) the flow is isentropic outside the boundary layer, (b) the Newtonian pressure formula holds, and (c) the local airfoil surface inclination relative to the free stream, θ, is everywhere small so that $\sin\theta \simeq \theta$ and $\cos\theta \simeq 1$. With these assumptions we may write

$$(22) \qquad \frac{T_e}{T_\infty} = \left(\frac{p_e}{p_\infty}\right)^{\frac{\gamma-1}{\gamma}}$$

and

$$(23) \qquad \frac{p_e}{p_\infty} = \frac{\rho_\infty V_\infty^2}{p_\infty}\left(\theta^2 + \epsilon\right)$$

where $\epsilon = p_\infty/\rho_\infty V_\infty^2 = 1/\gamma M_\infty^2$ is a small quantity. Substituting Equations (22) and (23) into Equation (21)

results in

$$(24)\quad \frac{\tau_w}{\rho_\infty V_\infty^2} = \left[\frac{\gamma(1-\alpha)}{(\gamma-1)}\frac{\mu_w}{\rho_\infty V_\infty c}(\theta^2+\epsilon)^{2-\frac{\gamma-1}{\gamma(1-\alpha)}}\right]^{\frac{1}{2}}\left[\int_0^{\frac{s}{c}}(\theta^2+\epsilon)^{1-\frac{\gamma-1}{\gamma(1-\alpha)}}\,d\left(\frac{s}{c}\right)\right]^{-\frac{1}{2}}$$

Noting that under the assumptions made $d(s/c) \simeq d(x/c)$ and $\tau_w \simeq \tau_x$ (the component of the viscous force in the free stream direction), and defining

$$Re_w = \frac{\rho_\infty V_\infty c}{\mu_w}$$

and

$$m = 1 - \frac{\gamma - 1}{\gamma(1 - \alpha)}$$

we may write the local frictional drag as

$$(25)\quad \frac{\tau_x}{\rho_\infty V_\infty^2} = (\theta^2 + \epsilon)^{\frac{m+1}{2}}\left[(1 - m)Re_w\int_0^{\frac{x}{c}}(\theta^2 + \epsilon)^m\,d\left(\frac{x}{c}\right)\right]^{-\frac{1}{2}}$$

FINAL DRAG EXPRESSION

With the aid of Equation (25) the total drag of one

surface of an airfoil may, in terms of the drag coefficient, be written

$$(26)\quad C_D = 2\int_0^1\left[\frac{(p_e - p_\infty)\theta}{\rho_\infty V_\infty^2} + \frac{\tau_w}{\rho_\infty V_\infty^2}\right]d\left(\frac{x}{c}\right)$$

Using the previous assumptions as to local pressure together with Equation (25) the drag coefficient becomes

$$(27)\quad C_D = 2\int_0^1\left\{\theta^3 + (\theta^2 + \epsilon)^{\frac{m+1}{2}} \cdot \left[(1 - m)Re_w\int_0^{\frac{x}{c}}(\theta^2 + \epsilon)^m\,d\left(\frac{x}{c}\right)\right]^{-\frac{1}{2}}\right\}d\left(\frac{x}{c}\right)$$

This equation (or one similar to it if other pressure laws had been used) is the basic equation for the class of optimization studies in which we are interested. We seek that distribution of airfoil slope $\theta(x/c)$ which will minimize the drag coefficient given by Equation (27) subject to any other constraints such as fixed lift, fixed center of pressure, fixed airfoil volume, etc. that we may desire.

OPTIMIZATION FOR MINIMUM DRAG AT SPECIFIED LIFT

In order to demonstrate the method, let us consider the following simplified problem. We assume an airfoil whose upper surface is a flat plate at zero angle of attack relative to the free stream velocity and we seek the shape of the lower surface which will minimize the drag while at the same time develop a required lift (see Figure 2). Also, for simplicity in our example, although it is not necessary, we assume that the base drag may be neglected. Our problem is then the following: We seek the function $\theta(x/c)$ which minimizes the integral

$$C_D = 2\int_0^1 \left\{\theta^3 + (\theta^2+\epsilon)^{\frac{m+1}{2}}\left[(1-m)Re_w\int_0^{\frac{x}{c}}(\theta^2+\epsilon)^m\, d\left(\frac{x}{c}\right)\right]^{-\frac{1}{2}}\right\} d\left(\frac{x}{c}\right)$$

while holding fixed the integral

$$C_L = 2\int_0^1 \theta^2 d\left(\frac{x}{c}\right) \tag{28}$$

The standard method for handling constraints of the type given in Equation (28) is through the use of Lagrangian

multipliers (see Reference 4). Introducing the Lagrangian multiplier λ, our problem becomes the minimization of the following integral

(29a)

$$I = C_D - \lambda C_L$$

$$= 2\int_0^1 \left\{(\theta^2+\epsilon)^{\frac{m+1}{2}}\left[(1-m)Re_w\int_0^{\frac{x}{c}}(\theta^2+\epsilon)^m d\left(\frac{x}{c}\right)\right]^{-\frac{1}{2}} + \theta^3 - \lambda\theta^2\right\} d\left(\frac{x}{c}\right)$$

$$= 2\int_0^1 F d\left(\frac{x}{c}\right)$$

The standard form of the elementary problem of the calculus of variations is the minimization of an integral of the form $I = \int F(y, y', x)dx$. The corresponding functional relationship between y and x which results in a stationary value of I is a second order differential equation (The Euler equation). If, however, the independent variable x is missing from the integrand so that the integral to be made stationary is $I = \int F(y, y')dx$, then

the first integral of the Euler equation may be written explicitly and a first order differential equation for the relationship between y and x is obtained. The integral in Equation (29) can be cast into this latter simple form by means of the transformation

$$\xi = \int_0^{\frac{x}{c}} (\theta^2 + \epsilon)^m \, d\left(\frac{x}{c}\right) \tag{30}$$

The derivative of this expression is simply

$$\xi' = (\theta^2 + \epsilon)^m \tag{31}$$

Insertion of these expressions for ξ and ξ' into Equation (29a) yields

(29b)

$$I = \int_0^1 \left\{ (\xi')^{\frac{m+1}{2m}} \left[(1-m) Re_w \xi \right]^{-\frac{1}{2}} + \left[(\xi')^{\frac{1}{m}} - \epsilon \right]^{\frac{3}{2}} - \lambda \left[(\xi')^{\frac{1}{m}} - \epsilon \right] \right\} d\left(\frac{x}{c}\right)$$

$$= \int_0^1 F(\xi, \xi') d\left(\frac{x}{c}\right)$$

The first order Euler equation which minimizes this

transformed integral can be written (see Reference 4)

$$\xi' \left(\frac{\partial F}{\partial \xi'} \right) - F = \text{constant} = C_1 \tag{32}$$

F being the integrand of Equation (29b). Equation (32) can be solved for ξ as a function of ξ', C, and λ. Furthermore, since ξ' is related to θ by Equation (31), ξ can be alternately expressed in terms of the original parameters. The resulting optimum shape is given by

$$\xi = \frac{(1 - m)(\theta^2 + \epsilon)^{m+1}}{Re_w \left[(2m - 3)\theta^3 + 2\lambda(1 - m)\theta^2 - 3\epsilon\theta + 2(\lambda\epsilon + mC_1) \right]^2} \tag{33}$$

The relationship between the local airfoil surface slope θ and the chordwize position x/c may be found as follows. Noting that

$$\xi' = \frac{d\xi}{d(x/c)} = \frac{d\xi}{d\theta} \frac{d\theta}{d(x/c)} = (\theta^2 + \epsilon)^m$$

we have

$$d(x/c) = (\theta^2 + \epsilon)^{-m} \left(\frac{d\xi}{d\theta}\right) d\theta$$

Evaluating $d\xi/d\theta$ by means of Equation (33) and integrating one obtains the "airfoil equation"

$$(34)\ \frac{x}{c} = \frac{2(1-m)}{Re_w} \int_{\theta_{\ell.e.}}^{\theta} \Big\{ (2-m)(3-2m)\theta^4 - 2(1-m)^2\theta^3 + 9\epsilon(1-m)\theta^2 + 2\Big[(3m-1)\lambda\epsilon + m(m+1)C_1\Big]\theta + 3\epsilon^2 \Big\} \cdot \Big[(2m-3)\theta^3 + 2\lambda(1-m)\theta^2 - 3\epsilon\theta + 2(\lambda\epsilon + mC_1)\Big]^{-3} d\theta$$

where $\theta_{\ell.e.}$ is the initial slope of the airfoil at its leading edge $(x/c = 0)$.

BOUNDARY CONDITIONS

To complete the solution for a particular airfoil, three constants must be evaluated $\theta_{\ell.e.}$, C_1, and λ.

The parameter λ is chosen so as to adjust the lift on the airfoil to the desired value. In making solutions it is convenient to choose several values of λ arbitrarily until a relationship between λ and the resulting lift coefficient is established. Thus, the two constants that must be evaluated in terms of the boundary conditions at the leading and trailing edges are $\theta_{\ell.e.}$ and C_1.

At the trailing edge of the airfoil neither a trailing edge slope nor a trailing edge position is specified so that a natural boundary condition must be applied. This natural boundary condition requires that at the trailing edge

$$\left(\frac{\partial F}{\partial \xi'}\right)_{t.e.} = 0$$

From the Euler equation (Equation (32)) it is evident that

$$C_1 = -F_{t.e.} = -(\theta_{t.e.} + \epsilon)^{\frac{m+1}{2}} \Big[(1-m)Re_w \xi_{t.e.}\Big]^{-\frac{1}{2}} - \theta_{t.e.}^3 + \lambda\theta_{t.e.}^2$$

or using Equation (33).

$$(35)\quad C_l = \left[(2 - m)\theta^3_{t.e.} - \lambda(1 - m)\theta^2_{t.e.} + 3\epsilon\theta_{t.e.} - 2\lambda\epsilon\right](1+m)^{-1}$$

The slope at the trailing edge $\theta_{t.e.}$ is obtained from the airfoil equation (Equation (34)) evaluated at the trailing edge i.e. at $x/c = 1$. Equation (35) is thus seen to be a relationship between C_l and $\theta_{\ell.e.}$.

The determination of the proper leading edge slope $\theta_{\ell.e.}$ is somewhat more complicated and far more interesting. At the leading edge $(x/c = 0)$ a singularity appears in the original expression to be minimized (Equation (29a)). This singularity is associated with the singularity in local shearing stress caused by the assumption of zero boundary layer thickness at the leading edge. The singularity is an integrable one and we may examine the behavior of the integrand of the integral to be minimized in the vicinity of the leading edge by assuming the leading edge slope to be fixed for some small but finite length Δx. With this assumption the integrand becomes

$$F = \theta^3_{\ell.e.} + \left[\frac{\theta^2_{\ell.e.} + \epsilon}{(1 - m)Re_w(\Delta x/c)}\right]^{\frac{1}{2}} - \lambda\theta^2_{\ell.e.}$$

It is clear that for small $\Delta x/c$ the square bracketed term can dominate the integrand. Just as it is written, the numerator of the term in square brackets is positive definite, so that the integrand would be minimized by choosing $\theta_{\ell.e.} = 0$. A moments reflection on the physical nature of the problem immediately indicates that we should be able to do better than this. The term $\theta^2_{\ell.e.} + \epsilon$ actually represents the non-dimensional local pressure $p_e/\rho_\infty V^2_\infty$. As we have written the usual Newtonian pressure formula we have not permitted non-dimensional pressures lower than $\epsilon = p_\infty/\rho_\infty V^2_\infty$. Since by using negative θ according to the convention shown in Figure 2 pressures lower than p_∞ are possible, a more complete formulation of the problem should permit lower drags if negative leading edge θ were chosen. Unfortunately such a choice would either cause the thickness of the airfoil to become negative or require a finite thickness of the leading edge. The first possibility is not permissible while the second possibility, that of starting the body

with a finite leading edge radius, requires the considerably more extended analysis necessary for a blunt airfoil. Such an analysis has not as yet been completed so that for the present we will consider the strictly mathematical problem of minimizing the integral as it is written in Equation (29a) and choose $\theta_{t.e.} = 0$. We will return to a discussion of the possibility of finite leading edge thicknesses in a later section of this paper.

2. SOLUTION FOR OPTIMUM SHARP AIRFOIL

As we have seen in the previous section, the shape of the optimum lower surface for a sharp airfoil having a given lift is given by the following expressions

$$(34a)\quad \frac{x}{c} = \frac{2(1-m)}{Re_w}\int_0^{\theta}\Big\{(2-m)(3-2m)\theta^4-2(1-m)^2\theta^3+9\epsilon(1-m)\theta^2 + 2\Big[(3m-1)\lambda\epsilon+m(m+1)C_1\Big]\theta+3\epsilon^2\Big\} \cdot\Big[(2m-3)\theta^3+2\lambda(1-m)\theta^2-3\epsilon\theta+2(\lambda\epsilon+mC_1)\Big]^{-3} d\theta$$

and

$$(35a)\quad C_1 = \Big[(2-m)\theta^3_{t.e.} - \lambda(1-m)\theta^2_{t.e.} + 3\epsilon\theta_{t.e.} - 2\lambda\epsilon\Big](1+m)^{-1}$$

If various values of λ are assumed the physical characteristics of each optimum airfoil so derived are obtained from the following formulae

$$(28a)\quad C_L = \int_0^{\theta_{t.e.}} \theta^2\Big[\frac{d(x/c)}{d\theta}\Big]\, d\theta$$

and

$$(27a)\quad C_D = 2\int_0^{\theta_{t.e.}} \Big\{\theta^3+(\theta^2+\epsilon)^{\frac{m+1}{2}}\Big[(1-m)Re_w\xi\Big]^{-\frac{1}{2}}\Big\}\frac{d(x/c)}{d\theta}\, d\theta$$

where ξ is given by Equation (33). The lower surface coordinate is given by

$$(36)\quad z/c = \int_0^{\theta} \theta\, \frac{d(x/c)}{d\theta}\, d\theta$$

As a typical example of the characteristics of a family of optimum airfoils obtained in the above manner, there is presented in Table 1 the results of a series of computations carried out for the purpose of designing a model for wind tunnel test. The Mach number considered was 17.5, the free stream Reynolds number $Re_\infty = 77{,}200$, the wall to stagnation temperature ratio $T_w/T_e^0 = 0.075$ so that $Re_w = 24{,}000$, and the ratio of specific heats for the flow about the model equal to 1.4. For these conditions the parameters m and ϵ are 0.646 and 0.00234 respectively. As mentioned before the upper surface is flat and under the conditions chosen has a drag coefficient of 0.00210. The aerodynamic characteristic shown in Table 1 are for both the lower surface alone as well as for both surfaces.

Table 1. Characteristics of Family of Optimized Flat-topped Sharp Airfoils
($M = 17.5$, $Re_w = 24{,}000$, $T_w/T_e^0 = 0.075$)

λ	C_L	$C_{D_{lower}}$	L/D_{lower}	L/D_{total}
0.150	0.0038	0.00165	2.33	1.02
0.175	0.0094	0.00264	3.56	1.99
0.200	0.0158	0.00406	3.89	2.57
0.225	0.0231	0.00584	3.96	2.91
0.250	0.0303	0.00774	3.92	3.08
0.300	0.0566	0.01509	3.76	3.30

The results given in Table 1 are also shown in Figure 3, where the lift over drag ratio for both the lower surface and for both surfaces are plotted as a function of lift coefficient. Also shown in Figure 3 for comparison are the L/D vs. C_L curves for an airfoil having a straight lower surface. It may be seen from Figure 3 that, at a lift coefficient of approximately 0.02, the improvement in L/D obtained by optimizing the lower surface is approximately 24 per cent. At higher lift coefficients where the pressure drag is a more important portion of the total drag this improvement falls off as expected. At a lift coefficient of 0.05 where the L/D of the optimized family is roughly a maximum and equal to 3.3, the improvement over the straight surface configuration is approximately 12 1/2 per cent.

In Figure 4 the shape of the lower surface of these optimized airfoils is illustrated by the specific example of the optimized airfoil designed for a lift coefficient of 0.0303. Both the actual airfoil shape as well as the distribution of local slope as a function of chordwize position are plotted. It is immediately apparent that in the minimization procedure the lift on the airfoil is

redistributed in such a way that no lift is carried where the boundary layer has no thickness, and in general on these airfoils, lift is carried after the boundary layer thickness has achieved a certain thickness which depends on the design lift coefficient. Notice that by lowering the lift carried at the leading edge, the resulting lower pressure allows the boundary layer to grow more rapidly.

The airfoil shown in Figure 4 has been built and is due to be tested in the very near future at the design conditions. It is unfortunate that these test results are not available for comparison with theory at this time.

3. DISCUSSION AND RECOMMENDATIONS

It is evident from this discussion of the optimization of airfoils when both pressure and viscous drag is considered that many interesting questions remain to be investigated. Two questions arise which are very closely related. Both are connected with the behavior of the boundary at the leading edge of the airfoil. Firstly, we notice that the most radical departures from inviscid

optimum body shape take place at the leading edge where the Reynolds numbers are very low and where conventional interaction between the boundary layer and the pressure distribution may take place. This question may be easily disposed of by noting that the solution we have obtained calls for a particular pressure distribution and hence a particular rate of growth of the boundary layer. To take the interaction effect into account, it is merely necessary in finding the optimum body shape to subtract the computed displacement thickness of the required boundary layer growth from the surface obtained by the analysis as given above. If this is done in the examples just given, we come back again to the problem of negative airfoil thickness or of finite leading edge radius.

The second question that is still to be answered is just the question of the choice of leading edge slope that was discussed previously and which also led to the problem of finite leading edge thickness.

It is interesting to speculate on this problem of finite leading edge thickness. The simple sharp leading edge analysis that allows the boundary layer thickness to approach zero at the leading edge, when applied to either

the upper or lower surface independently and with more accurate pressure formulae than were used in the present paper, indicates that the optimum shapes should have low pressure near the leading edges of both upper and lower surfaces. Thus the surfaces look somewhat as shown in the following sketch. It is obvious from this figure that if the two leading edges were put together, an airfoil of negative thickness would result. If they are not put together, an airfoil of finite leading edge thickness results and the whole method of analysis must be modified. Not only would one have to consider surfaces of large slope and thus only the streamwise components of the viscous drag, but also the vorticity generated by the strong bow shock in which a portion of the boundary layer would be submerged would have to be taken into account. In addition, we note that because of the large variations of local Mach number that would be encountered, the simplified form of the momentum integral equation would not be applicable. Because of the great difficulty of attacking this problem theoretically, it would seem that perhaps some experiments should be undertaken to see if a very small and properly designed bluntness could improve the L/D characteristics of

optimum upper surface

optimum lower surface

Typical upper and lower optimized surfaces when surfaces are considered independently.

supersonic or hypersonic airfoils at low Reynolds numbers. It is very hard for one used to working with flows at high Reynolds numbers to believe that an improvement could be made by such means. Nevertheless, if an improvement can be made in this manner, it would be a most interesting phenomenon. Alternatively, if an improvement cannot be made, the general features of the method outlined in this paper can be used to improve the L/D performance of airfoils when the viscous drag is an appreciable portion of the total drag.

REFERENCES

1. Von Karman, T. The Problem of Resistance in Compressible Fluids. Atti del Convegno della Fondazione Alessandro Volta 1935, pp. 223-326, 1936.

2. Eggers, A.J., Resnikoff, M.M., and Dennis, D.H. Bodies of Revolution Having Minimum Drag at Supersonic Airspeeds. NACA Report No. 1306 (1957). Supersedes NACA Tech. Note No. 3666 (1956).

3. Hayes, Wallace D. Hypersonic Flow Theory. pp. 93-109 Academic Press, 1959.

4. Weinstock, R. Calculus of Variations. McGraw-Hill Book Company, Inc., New York (1952).

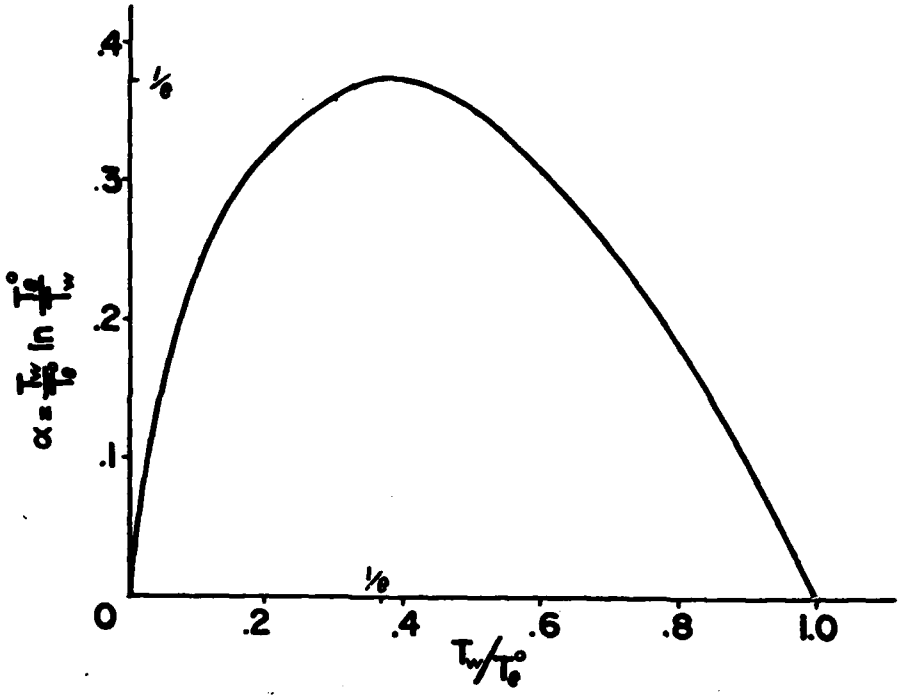

Fig 1. Behavior of the wall temperature parameter α as a function of the wall to stagnation temperature ratio.

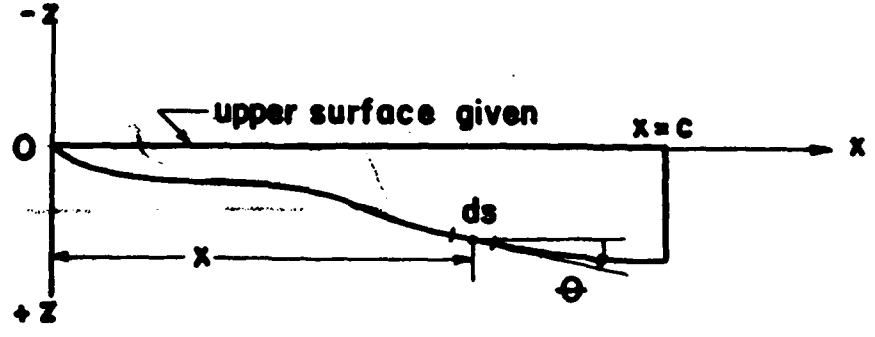

Fig.2. Simplified optimization problem considered.

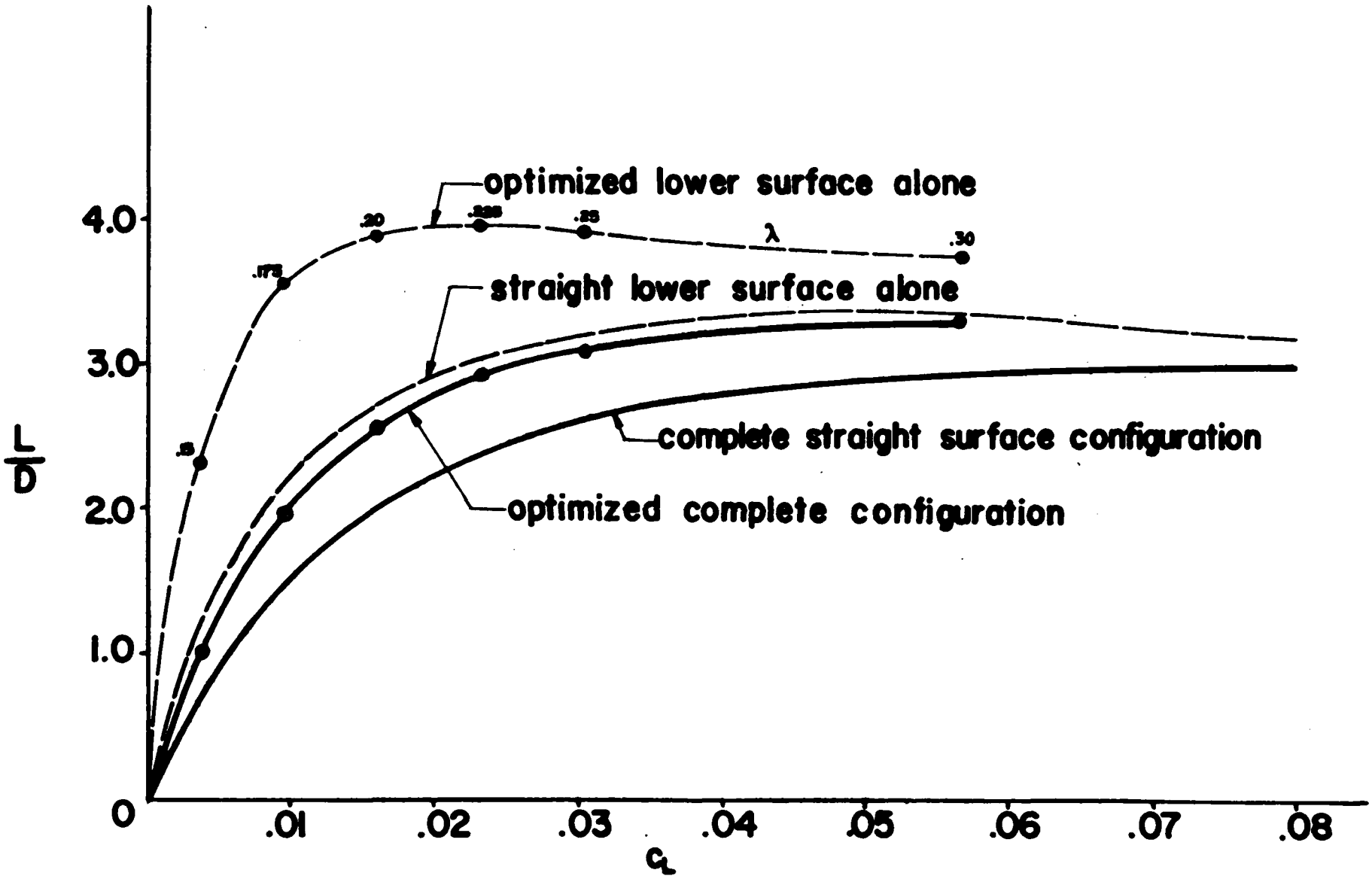

Fig. 3. L/D vs. c_L curves for a Family of Optimized Flat-topped Sharp Airfoils.
($M = 17.5$, $Re_w = 24{,}000$, $T_w/T_0^\circ = 0.075$)

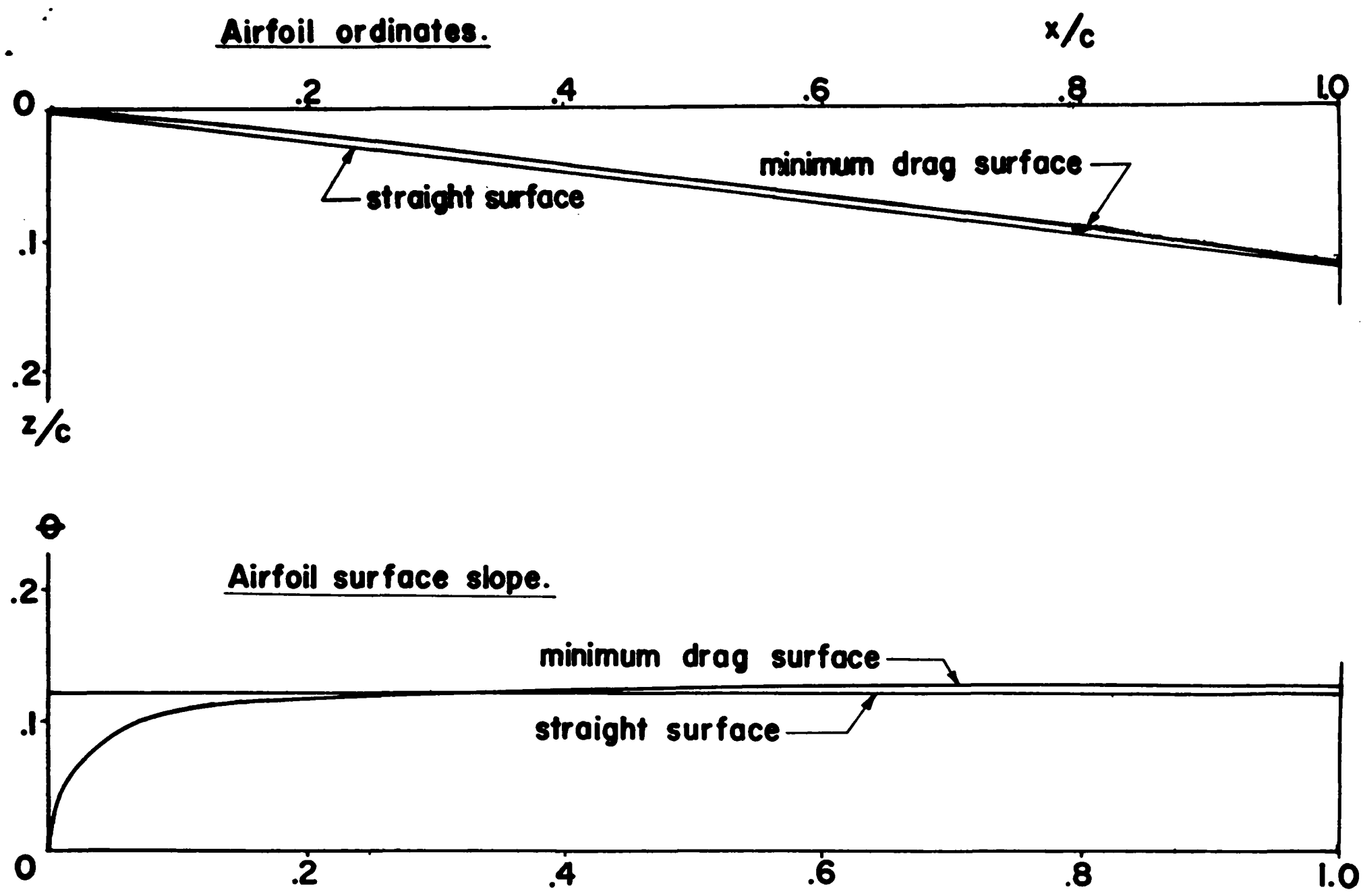

Fig.4. Optimized Flat-Topped Sharp Airfoil Shape.
($M=17.5$, $Re_w=24{,}000$, $T_w/T_0^\circ=0.075$, $c_L=0.0303$)